Publications

11-27-2001

Reflection of a Long-period Gravity Wave Observed in the Nightglow over Arecibo on May 8–9, 1989?

Michael P. Hickey Ph.D.
Embry-Riddle Aeronautical University, hicke0b5@erau.edu

Follow this and additional works at: https://commons.erau.edu/publication

Part of the Atmospheric Sciences Commons

Reflection of a long-period gravity wave observed in the nightglow over Arecibo on May 8–9, 1989?

Michael P. Hickey

Department of Physics and Astronomy, Clemson University, Clemson, South Carolina, USA

Abstract. During the Arecibo Initiative for Dynamics of the Atmosphere (AIDA) campaign in 1989 a characteristic of gravity wave perturbations observed in mesopause region airglow emissions was that airglow brightness fluctuations and airglow-derived temperature fluctuations often occurred either in phase or in antiphase. This stimulated the development of a theory suggesting that such in-phase fluctuations were most probably the result of strong reflections occurring in the mesosphere and lower thermosphere region. Recent examination of a particular wave event and application of simple WKB-type theory has appeared to support this hypothesis. Here we use a full-wave model and a WKB-type model, each coupled with a chemical-airglow fluctuation model describing O_2 atmospheric and OH Meinel airglow fluctuations, to assess the strength of wave reflection and also to explicitly calculate the phase difference between the airglow brightness and the temperature fluctuations. Our results suggest that reflection is not strong for the particular wave event, and the model produces fairly large phase differences between the airglow brightness and the temperature fluctuations ($\sim 35°$ and $\sim 134°-165°$ for the O_2 atmospheric and OH airglow emissions, respectively). These results are not particularly sensitive to the nominal mean winds used in the simulations. There is an instance when a region of minimum refractive index occurs directly above a region in which reflection is strongest, suggesting that the two are related. However, the reflection does not appear to be strong. Our results suggest that chemical effects can account for the inferred phases of the observed airglow fluctuations and that effects associated with wave reflection appear to play a relatively minor role in the airglow fluctuations.

1. Introduction

It is well accepted that gravity waves perturb the airglow emission layers, leading to fluctuations in airglow brightness and in temperature derived from the airglow [e.g., *Taylor et al.*, 1987; *Hickey et al.*, 1997; *Schubert et al.*, 1991, 1999, and references therein]. *Krassovsky* [1972] was the first to attempt to relate the associated brightness fluctuations with temperature fluctuations, and the parameter that bears his name for this purpose is independent of wave amplitude for linear airglow disturbances. Physically, Krassovsky's ratio represents a complex transfer function relating the input temperature perturbation to the output brightness perturbation. An interesting feature of values of Krassovsky's ratio derived from observations is that often the airglow brightness and temperature appear to fluctuate either exactly in phase or exactly out of phase [see *Hines and Tarasick*, 1994, and references therein]. For internal gravity waves of very large vertical wavelength as well as for evanescent waves, the phase of Krassovsky's ratio (hereinafter referred to as $\varphi(\eta)$) should be either zero or π. However, observations [e.g., *Zhang et al.*, 1993a] suggest values of $\varphi(\eta) \approx 0$ for waves not having large vertical wavelengths. *Hines and Tarasick* [1994] explained this phenomenon as being due to wave reflection. If reflection is strong enough, standing wave behavior may result, leading to values of $\varphi(\eta) \approx 0$ or π.

One particularly relevant observation that has come under scrutiny is that of *Zhang et al.* [1993a]. On the night of May 8–9, 1989, during the Arecibo Initiative for Dynamics of the Atmosphere (AIDA) campaign, Zhang et al. observed a large-scale

gravity wave (period ~ 2 hours, horizontal wavelength ~ 1300 km) disturbance in the O_2 atmospheric airglow emission for which $\varphi(\eta) = 0$. Numerical modeling using a simple WKB analysis was unable to reproduce the observed phase [*Zhang et al.*, 1993b; *Hickey et al.*, 1993]. This led *Hines and Tarasick* [1994] to postulate and subsequently demonstrate that strong reflection could account for values of $\varphi(\eta)$ equal to either zero or π.

Walterscheid et al. [2000] reexamined this particular case. They used measured winds in the airglow region to demonstrate that the altitude region of minimum refractive index is also a region where the WKB approximation is expected to fail. Significantly, this occurs in the airglow region (~ 90 km) and suggests that reflection may indeed be significant and may be responsible for the small values of $\varphi(\eta)$ for the O_2 atmospheric airglow emission and the large values of $\varphi(\eta)$ for the OH airglow emission. As discussed by *Walterscheid et al.* [2000], observations by *Hecht et al.* [1993] of O_2 atmospheric brightness and OH Meinel (6-2) brightness revealed that the two emissions were fluctuating nearly out of phase with each other. Because airglow temperature fluctuations for the two emissions occurred almost in phase (within less than 30°), and derived values of $\varphi(\eta) \leq 0$ for the O_2 atmospheric and $\varphi(\eta) \approx 130°$ for the OH Meinel, *Walterscheid et al.* [2000] concluded that the out-of-phase relationship between OH Meinel and O_2 atmospheric brightness fluctuations was due to the out-of-phase relationship between OH Meinel temperature and brightness fluctuations. They conjectured that this out-of-phase relationship between OH Meinel temperature and brightness fluctuations was due to the strong influence of wave reflection in the region of the OH Meinel airglow layer. The study of *Walterscheid et al.* [2000] did not include a simulation of wave effects on the airglow, and so modeled values of $\varphi(\eta)$ were not derived. Consequently, the role of chemistry in the observed phase differences was not addressed. Other gravity wave events associated with the AIDA campaign have been analyzed and discussed by *Schubert et al.* [1999].

We use both a full-wave model and a WKB-type model to describe the dynamical gravity wave quantities in the mesosphere/lower thermosphere (MLT) region. The full-wave model allows us to assess the strength of reflection while also providing values of $\varphi(\eta)$ for several airglow emissions. The model has been used extensively to simulate the ducting of very short period gravity waves in the lower thermospheric thermal duct [*Walterscheid et al.*, 1999] while also including mean wind effects [*Hecht et al.*, 2001]. Using this model, these studies have been able to explain the observed seasonal variation of the preferred azimuths of gravity wave propagation. The full-wave model has also been used to perform a detailed study of the effects of these short-period ducted waves on the O_2 atmospheric airglow emission, with particular emphasis on the relation of ducting efficiency to values of $\varphi(\eta)$ [*Hickey*, 2001]. The WKB-type model is essentially that described previously by *Hickey et al.* [1993] and references contained therein. The WKB model does not include a reflected wave component, whereas the full-wave model does. Therefore significant differences between airglow fluctuation characteristics calculated using the two different models is indicative that reflection is strong.

It is the purpose of this paper to derive values of $\varphi(\eta)$ for the O_2 atmospheric airglow and the OH Meinel airglow for the large-scale gravity wave, described above, using our full-wave and WKB models and including the effects of mean winds and mean thermal gradients. The full-wave model will allow us to infer whether reflection is strong enough for this particular wave to produce values of $\varphi(\eta)$ which reasonably match the observed values. Further comparison with WKB-derived results should provide additional support for any inferences regarding the significance of reflection because the WKB model does not account for reflection. We should be able to definitively determine whether reflection is responsible for the small ($\sim 0°$) values of $\varphi(\eta)$ for the O_2 atmospheric airglow observed by *Zhang et al.* [1993a]. We will also be able to determine the extent to which reflection and chemistry are responsible for the observed values of $\varphi(\eta) \approx 130°$ for the OH (6-2) airglow emission by *Hecht et al.* [1993]. The layout of this paper is as follows: In section 2 we briefly discuss the numerical models used to study the wave, as well as the model input and output. Results are discussed in section 3. A brief discussion is given in section 4, and conclusions are presented in section 5.

2. Model Description

To simulate gravity wave propagation in a realistic atmosphere containing height-dependent winds, diffusion, and mean temperature gradients, we employ a full-wave model that has been described by *Hickey et al.* [1997, 1998, 2000a]. The model solves the linearized Navier-Stokes equations for steady-state waves propagating in a nonisothermal atmosphere, including the eddy and molecular diffusion of heat and momentum and horizontal mean winds. The lower boundary is the ground, and the upper boundary for the present simulations was set to 450 km altitude. We used 120,000 grid points, corresponding to a height resolution of 3.75 m.

Boundary conditions for the full-wave model have been extensively discussed in the above references. Essentially, the ground reflects waves, and at the upper boundary a radiation condition is applied using a dispersion equation given by *Hickey and Cole* [1987]. A sponge layer is also implemented at the upper boundary to absorb any waves that may be reflected due to a slight mismatch between full-wave and WKB-type solutions used during the implementation of the radiation condition [*Hickey et al.*, 2000a].

The WKB model has been described previously by *Hickey et al.* [1993] and in the references contained therein. The Navier-Stokes equations are solved using the approach of *Hickey and Cole* [1987], wherein a quartic dispersion equation is derived which includes molecular dissipation processes, and eddy dissipation in the manner described by *Hickey* [1988].

The output from each of these models is input to a steady-state, linear chemistry model that simulates the effects of gravity waves on minor species and related airglow volume emission rates and airglow brightness as viewed in the nadir from the ground. We consider two different chemical schemes and related airglow emissions. The first scheme we consider is that which describes the O_2 atmospheric nightglow, and the chemical kinetic parameters we use have been described by *Hickey et al.* [1993] and *Hickey and Walterscheid* [1999]. The second scheme we consider is the OH Meinel (6-2) nightglow, and the kinetic parameters we use are described in Appendix A. Note that the (6-2) band of the OH Meinel was measured by *Hecht et al.* [1993]. We calculate the complex Krassovsky's ratio using the approach discussed by *Schubert and Walterscheid* [1988].

2.1. Model Input

The mean atmospheric state (temperature, density, pressure, etc.) is specified using the MSIS-90 model [*Hedin*, 1991]. This model requires geographic position (Arecibo Observatory, 18.35° N, 66.75° W), solar ($F_{10.7} = 205$), and geomagnetic ($a_p = 10$) indices, and day number (May 8–9 = 128) as input. The nominal eddy diffusion coefficients are based upon a profile due to *Strobel* [1989] and have large values in the airglow region (the momentum diffusivity maximizes with a value of 100 $m^2 s^{-1}$ at 80 km altitude). The Prandtl number is equal to 3.

The undisturbed profile of the volume emission rate (VER) for the O_2 atmospheric airglow is shown in Figure 1. The O_2 atmospheric VER peaks near 91.4 km altitude with a value of 3.3×10^8 photons $m^{-3} s^{-1}$. Minor species number densities used to calculate the OH Meinel VER are taken from *Garcia and Solomon* [1985], as supplied by F. Garcia (private communication, 1990). The OH Meinel (6-2) VER peaks near 88.4 km altitude with a value of 2.5×10^9 photons $m^{-3} s^{-1}$. Note that our VER values are high because they represent the integrated VER over the entire band.

The mean temperature is shown in Figure 2. The mesopause is fairly broad and high, with the minimum value of ~ 171.5 K occurring at ~ 97 km altitude. This is about 6 km above the altitude of peak O_2 atmospheric VER and about 9 km above the altitude of peak OH VER.
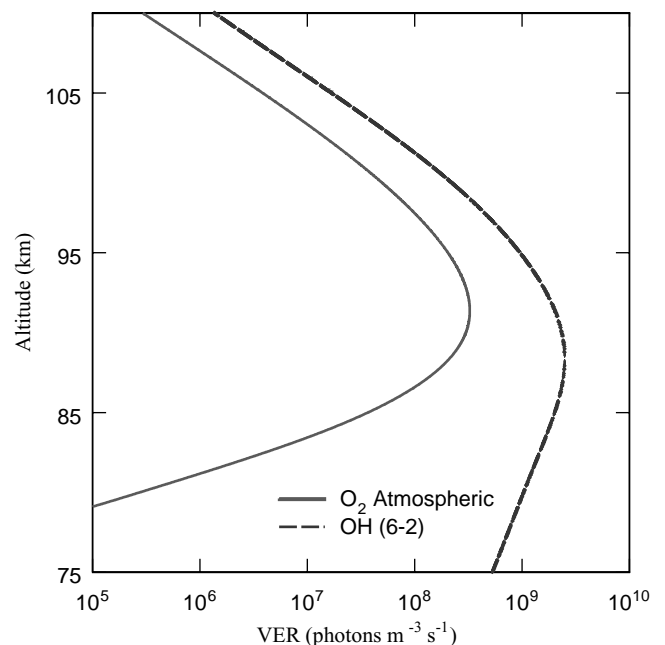

Figure 1. Calculated volume emission rates for the O_2 atmospheric and OH (6-2) Meinel airglow emissions using the nominal chemistry and mean state parameters described in the main text.
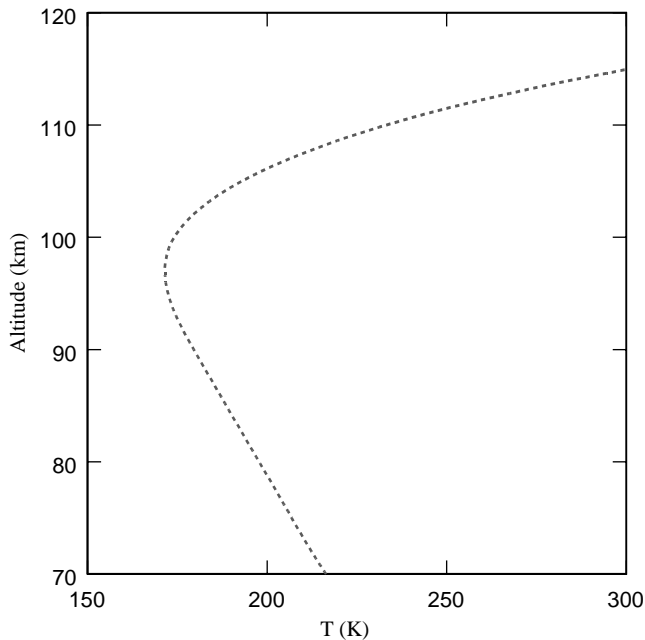
Figure 2. Mean atmospheric temperature used in the computations.

We investigate the effects of winds using several different mean wind profiles in our computations. The first is specified using the wind profiles presented by *Walterscheid et al.* [2000, Figure 6] (valid for 0200-0300 LT). These winds are based on Geospace Meteor Radar measurements obtained at ~1 hour temporal resolution and a vertical resolution (after averaging) of ~2 km (see *Walterscheid et al.* [2000] for a more detailed discussion of these winds). We also consider the possibility that the overlying lower thermospheric winds could be causing strong wave reflection. Accordingly, we also use the horizontal wind model (HWM) [*Hedin et al.*, 1996] to define the mean winds throughout the atmosphere for May 8/9. Tidal variations are quite strong in the lower thermosphere, and therefore the mean winds and the associated wave reflection may depend quite sensitively on local time [*Hecht et al.*, 2001]. Therefore for the HWM winds we selected three different local times (0000, 0200, and 0400 LT), which corresponds to the time period analyzed in detail by W2000. The background winds are shown in Figure 3, where the meridional wind (Figure 3a) is positive due south, as in our models. The mean winds due to W2000 were adjusted here to approach zero at altitudes above 100 km and below 80 km. The HWM winds were adjusted so that in the troposphere they approach values of zero, while in the upper thermosphere, their gradients approach zero. It is apparent that the HWM winds do not, in general, agree well with the measured winds, as represented by the W2000 curves. As it transpires, our results are not too sensitive to the particular wind profile used because the phase speeds of the waves we consider $(110-160 \text{ m s}^{-1})$ are significantly greater than the wind speeds.

The required wave inputs for the dynamical models are wave period, horizontal wavelength, and azimuth of propagation. These inputs are taken from *Zhang et al.* [1993a] (hereinafter referred to as Z93) and *Walterscheid et al.* [2000] (hereinafter referred to as W2000). Z93 deduced a wave period (T) of 135 min, a horizontal wavelength (λ_x) of 1300 km, and a direction of propagation (φ_{az}) 60° east of south for the gravity wave of interest. The same wave has been further studied by W2000, who concluded that strong wave reflection was occurring as a result of Doppler shifting associated with the mean winds in the airglow region. W2000 deduced a set of best fit parameters giving $T = 2$ hours, $\lambda_x = 800$ km,

and $\varphi_{az} = 45°$ east of south. These two sets of wave parameters are summarized in Table 1. Note that the phase speeds (V_{px}) of these waves are 160.5 m s^{-1} (for Z93) and 111.1 m s^{-1} (for W2000).

2.2. Model Output

The full-wave and WKB models output altitude profiles of amplitude and phase for the horizontal velocity components $(u'$ and $v')$, the vertical velocity (w'), the temperature perturbation (T') and the pressure perturbation (p'). As previously stated, the output from these models is input to the two chemistry models so that we
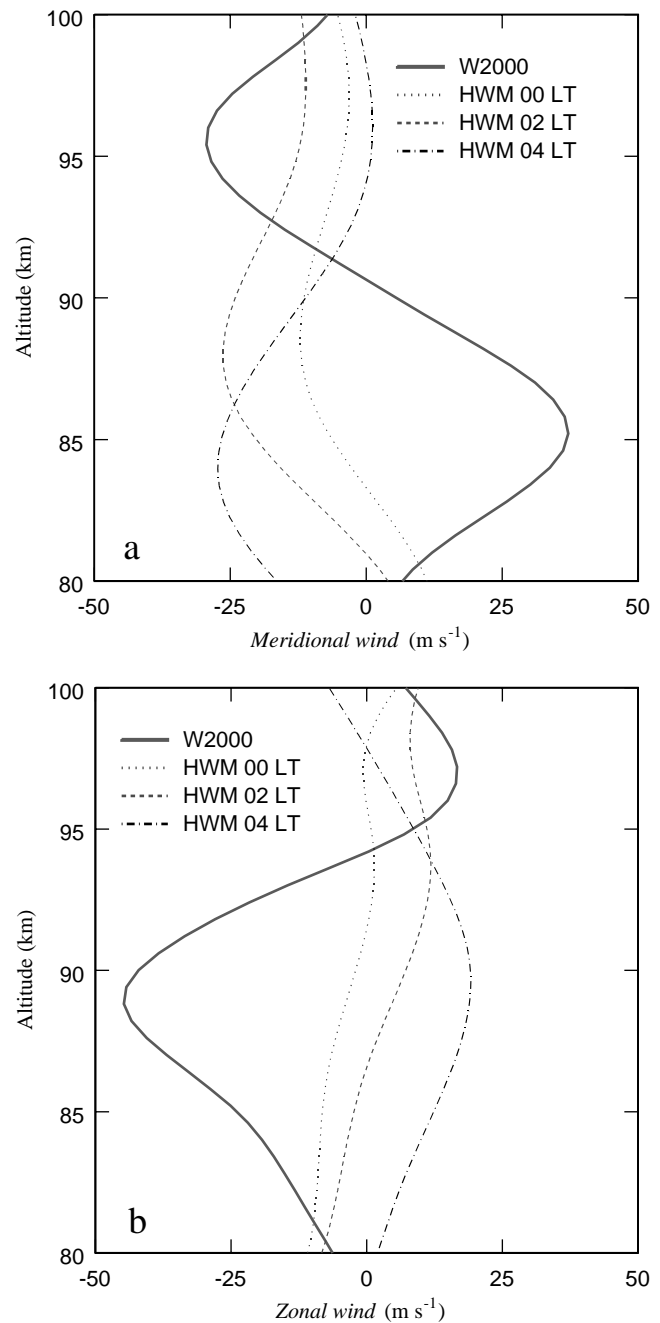

Figure 3. (a) Meridional winds and (b) zonal winds from W2000 (see text for details) and the horizontal wind model at three local times shown in the figure. The meridional wind is taken as positive due south, and the zonal wind is positive due east.

Table 1. Wave Parameters of *Walterscheid et al.* [2000] and *Zhang et al.* [1993a][a]

	λ_x (km)	T (min)	φ_{az} (deg)	V_{px} (m s^{-1})
Walterscheid et al.	800	120	135	111.1
Zhang et al.	1300	135	120	160.5

[a]Note that the azimuth of propagation follows the convention wherein zero corresponds to due north, and azimuth increases in a clockwise direction therefrom. See text for details.

can calculate the phase of Krassovsky's ratio (denoted $\varphi(\eta)$) for the O$_2$ atmospheric and OH Meinel airglow emissions.

In addition to calculating $\varphi(\eta)$, we also calculate the refractive index m_{WKB}^2 given by [*Hines*, 1960; *Einaudi and Hines*, 1971]

$$m_{WKB}^2 = \frac{k^2}{\Omega^2}(N^2 - \Omega^2) - \frac{1}{4H^2} + \frac{\Omega^2}{C^2}, \qquad (1)$$

where k is the horizontal wave number, H is the atmospheric pressure scale height, C is the sound speed, and N is the nonisothermal Brunt-Vaisala frequency. Ω is the intrinsic (i.e., Doppler shifted) wave frequency, given by $\Omega = \omega - \underline{k} \cdot \underline{U}$, where ω is the extrinsic (observable) wave frequency (assumed to be much greater than the inertial frequency), $\underline{k}$ is the horizontal wave number vector, and $\underline{U}$ is the mean wind. Also, $N^2 = (\gamma - 1 + \gamma dH/dz)g^2/C^2$ is the square of the Brunt-Vaisala frequency. Additional useful relations are $H = RT/Mg$ and $C^2 = \gamma gH$, where R is the universal gas constant, T is the mean temperature, M is the mean molecular weight, g is the gravitational acceleration, and γ is the usual ratio of specific heats. Also, the vertical wavelength is given by $\lambda_z = 2\pi/m_{WKB}$. Note that because m_{WKB}^2 is evaluated using equation (1), it is model independent.

We also calculate a refractive index, m_{fw}^2, using the local phase gradient of the temperature perturbations ($\varphi_{T'}$) output from the full-wave model, as follows:

$$m_{fw}^2 = \left(\frac{d\varphi_{T'}}{dz}\right)^2, \qquad (2)$$

where z is altitude. If reflection were important, significant differences between values of m_{WKB}^2 and m_{fw}^2 should occur. It is important to realize that when such differences occur, values of m^2 derived using (2) should be used instead of values derived using (1). Additionally, we note that values of m_{fw}^2 can be calculated using phases associated with other than the temperature perturbations, such as the velocity perturbations or the pressure perturbations. When that is done, one finds that the refactive indexes are all slightly different from one another (not shown), which is expected from a full-wave model (see, for example, the discussion by *Einaudi and Hines* [1971]). However, these differences are not large, and we choose to use the phase of the temperature perturbations, as in (2), simply to reduce the volume of results displayed.

To quantify the strength of wave reflection, we also examine the phase difference between vertical velocity perturbations and pressure perturbations derived from the full-wave model, which we denote $\varphi(w'p')$. When reflection is strong, one expects little or no vertical transport of energy, so w' and p' will be in approximate phase quadrature and $\varphi(w'p') \approx \pm \pi/2$. Large departures of $\varphi(w'p')$ from $\pm\pi/2$ signifies either weak or very inefficient reflection. Note that our measure of wave reflection, based on the phase quadrature of w' and p', may not be the best choice in the case of strong sheared flow because then the vertical energy flux is not necessarily zero [*Holton*, 1975, p.107]. It is, however, a reasonable and useful measure for our purposes. Because reflection is not accounted for in our WKB model we do not calculate the corresponding WKB-derived value of $\varphi(w'p')$.

3. Results

The phase of the temperature perturbation ($\varphi_{T'}$) is shown as a function of altitude for the W2000 wave and the Z93 wave in Figures 4a and 4b, respectively. An important feature of the results shown in both figures is that the gradient of $\varphi_{T'}$ changes slowly with increasing altitude. In particular, $\varphi_{T'}$ does not exhibit the behavior associated with waves that are subject to strong reflection: such waves typically exhibit values of $\varphi_{T'}$ whose gradients tend to depend strongly on altitude. For example, over relatively small height ranges, local gradients can vary appreciably, being large in one region and small in another [e.g., *Walterscheid et al.*, 1999, Figures 12 and 13]. The local vertical wavelengths (not shown) can
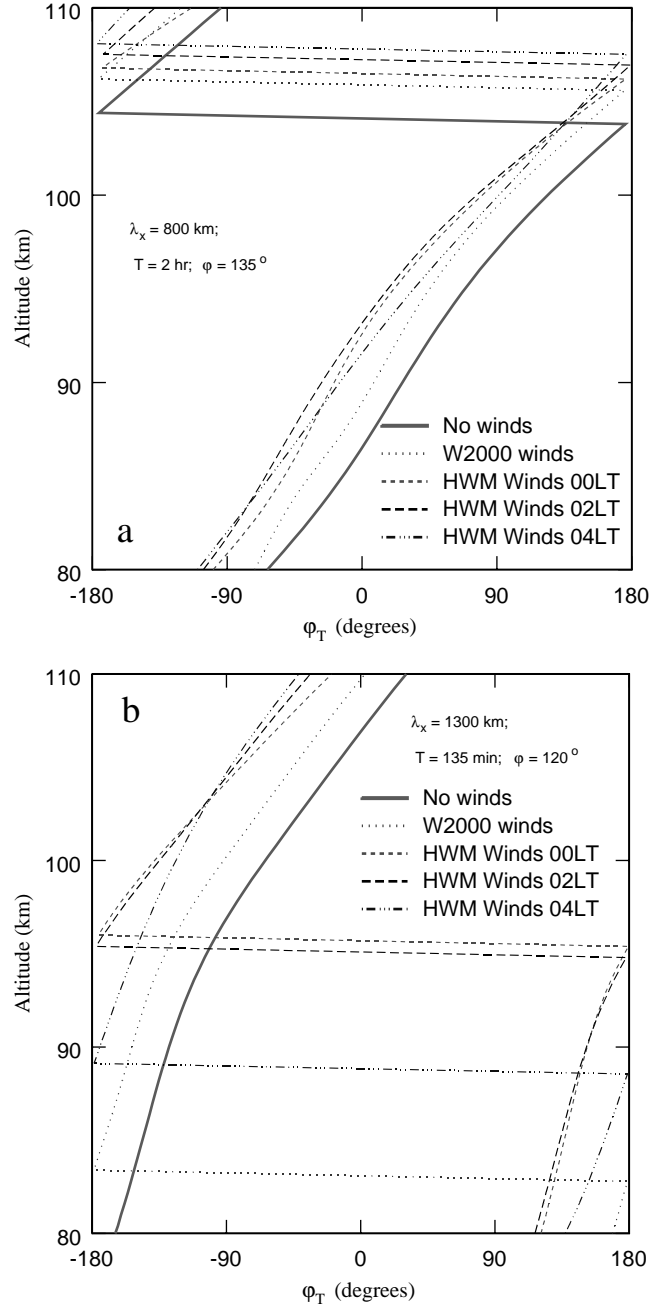
Figure 4. Phase of the temperature perturbation provided by the full-wave model plotted as a function of altitude and calculated without winds and using the winds shown in Figure 3 for (a) the W2000 wave and (b) the Z93 wave.
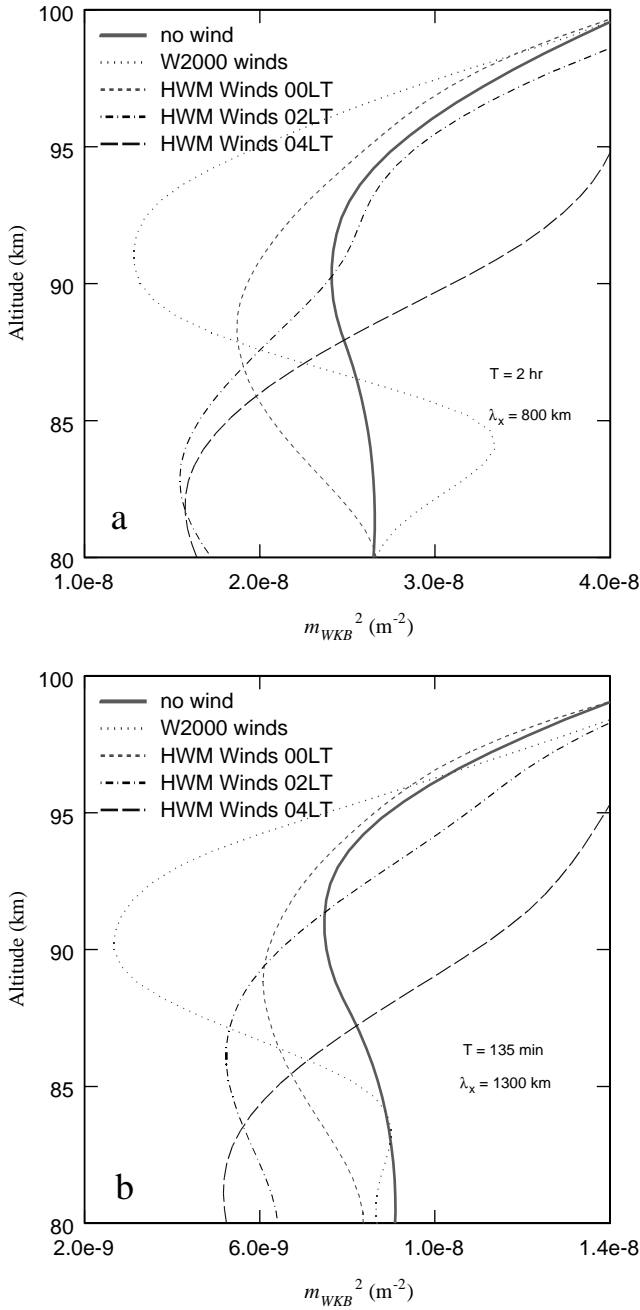
Figure 5. Refractive index based on equation (1) of the main text for (a) the W2000 wave and (b) the Z93 wave, calculated without winds and using the winds shown in Figure 3.

be estimated from the slope of $\varphi_{T'}$. Average values of λ_z over the 80–110 km altitude interval are ~33 and 67 km for the W2000 and Z93 waves, respectively. Therefore the Z93 wave has a vertical wavelength that is approximately double that of the W2000 wave.

The refractive index m_{WKB}^2 is calculated using (1) both with and without mean winds included and using either the W2000 set of wave parameters (Figure 5a) or the Z93 set of wave parameters (Figure 5b). For the W2000 wave parameters (Figure 5a), in the case of no winds, values of m_{WKB}^2 always exceed 2×10^{-8} m^{-2} in the height range of 80–100 km. The inclusion of winds modifies m_{WKB}^2, which achieves a minimum value of ~1.3×10^{-8} m^{-2} at ~91 km altitude when the W2000 winds are included. These results agree well with those of W2000, wherein a minimum in m_{WKB}^2 occurs at ~90 km altitude (see their Figure 9). What is

significant about these results is that m_{WKB}^2 never becomes negative for any of the winds considered.

The refractive index m_{WKB}^2 calculated using the Z93 set of wave parameters is shown in Figure 5b. At all altitudes these values of m_{WKB}^2 are smaller than the corresponding values shown in Figure 5a, because both the horizontal wavelength and the horizontal phase speed inferred by Z93 are significantly greater than those inferred by W2000. The minimum in m_{WKB}^2 occurs at ~90 km altitude with the W2000 winds, essentially in agreement with the results obtained using the W2000 set of wave parameters. However, as before, m_{WKB}^2 never becomes negative for any of the winds considered.

The refractive index, m_{fw}^2, is calculated using (2) both with and without mean winds included and using either the W2000 set of wave parameters (Figure 6a) or the Z93 set of wave parameters
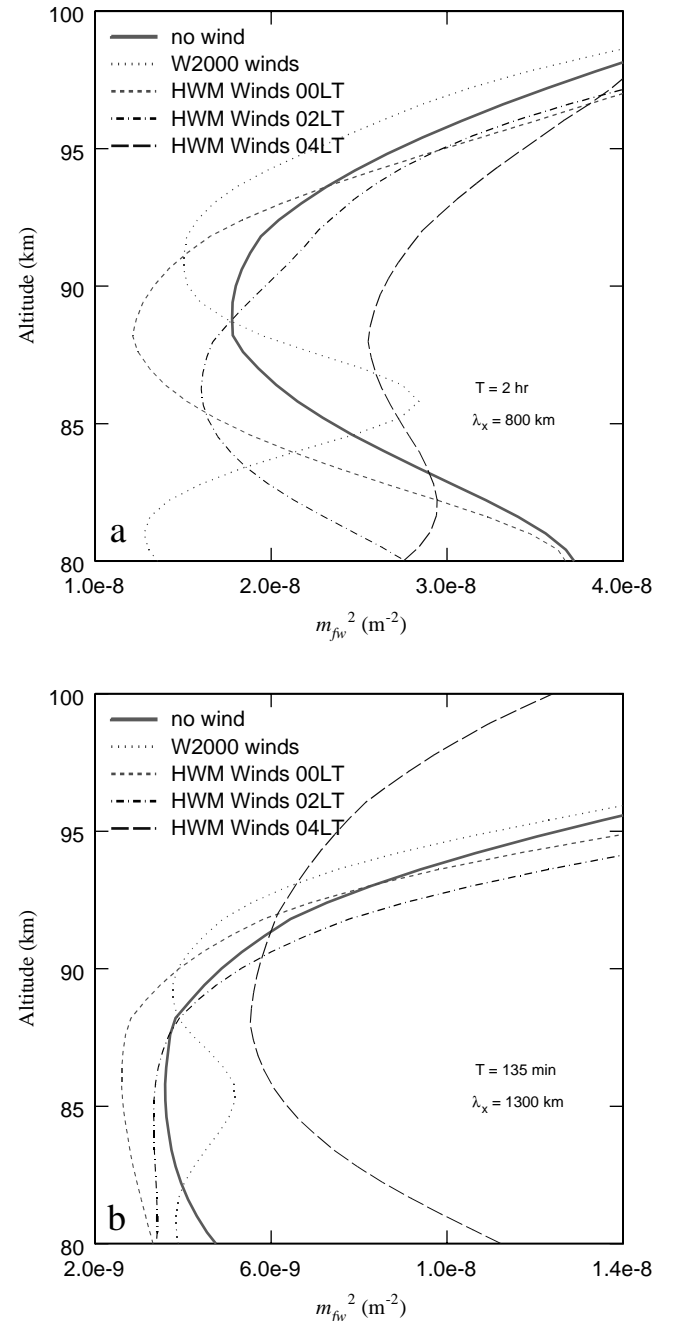

Figure 6. Similar to Figure 5 except using the full-wave model (equation (2) of the main text).
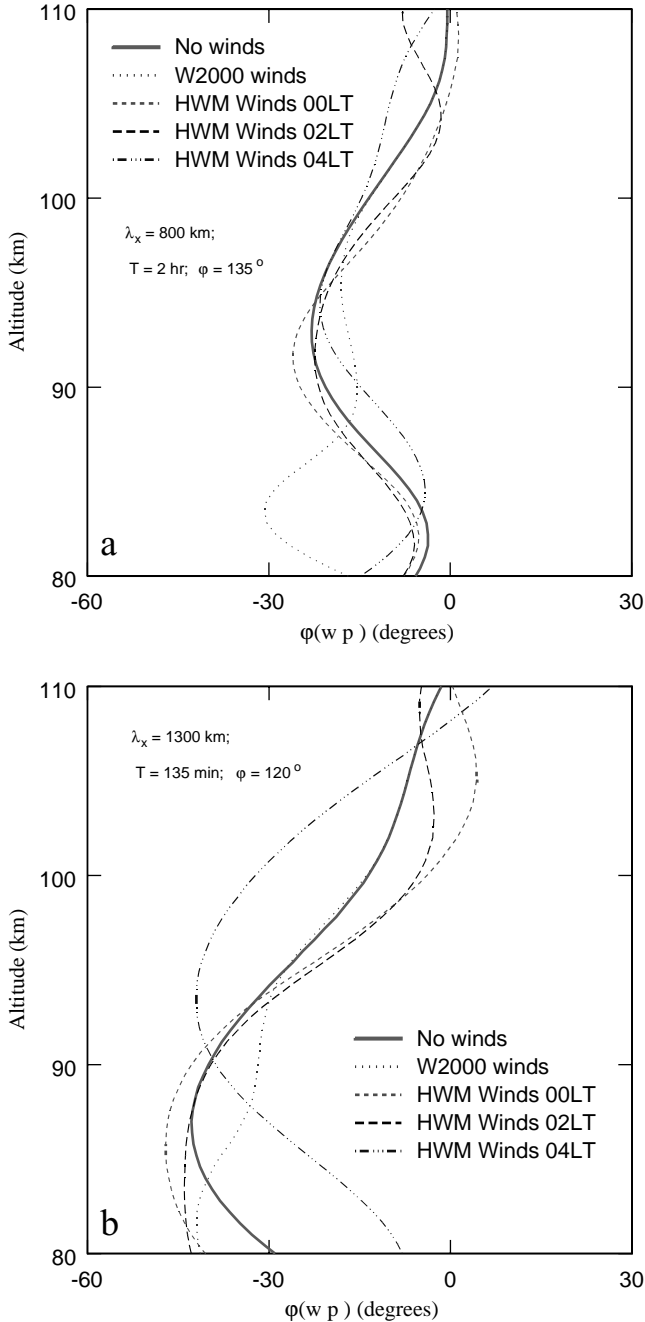
Figure 7. Phase differences between vertical velocity and pressure fluctuations as derived from the full-wave model for (a) the W2000 wave and (b) the Z93 wave, calculated without winds and using the winds shown in Figure 3.

tions. In particular, near 90 km altitude, the smallest values of m_{WKB}^2 occur for propagation in the W2000 winds, whereas the smallest values of m_{fw}^2 occur for propagation in the HWM winds evaluated at 0000 LT. Values of m_{WKB}^2 agree with values of m_{fw}^2 to within a factor of about 2.

Values of m_{fw}^2 obtained using the Z93 set of wave parameters are shown in Figure 6b . Once again, differences are seen between values of m_{WKB}^2 shown in Figure 5b and values of m_{fw}^2 shown in Figure 6b. As for the W2000 wave discussed previously, values of m_{WKB}^2 agree with values of m_{fw}^2 to within a factor of about 2. Below 90 km altitude, minimum values of m_{fw}^2 now occur for propagation in the HWM winds evaluated at 0000 LT. Another feature of these results is that values of m_{fw}^2 evaluated without winds are aproximately half the values of m_{WKB}^2 evaluated without winds over the altitude range $85-87$ km. This implies that reflection due to the nonisothermal character of the atmosphere must be stronger for the Z93 wave than for the W2000 wave (compare Figure 5a with Figure 6a).

Using the two sets of wave parameters and the different wind profiles, we have also calculated the phase difference between vertical velocity perturbations and pressure perturbations output from our full-wave model, which we denote $\varphi(w'p')$. These results are shown in Figure 7a (for the W2000 set of wave parameters) and Figure 7b (for the Z93 set of wave parameters). The value of $\varphi(w'p')$ for the windless case is not significantly changed by the inclusion of mean winds for the W2000 set of wave parameters (Figure 7a), except perhaps at the lowest altitudes shown for the W2000 winds, where $\varphi(w'p')$ achieves values as small as about $-35°$. However, values of $\varphi(w'p')$ are never close to $\pm\pi/2$, and so these winds do not appear to greatly influence wave reflection for this set of wave parameters. Nonetheless, the feasibility that some reflection is occurring from altitudes centered near 90 km (as inferred by W2000 and our m^2 results shown in Figures 5a and 6a) and, subsequently, affecting $\varphi(w'p')$ in the region directly below this altitude is supported by our results for the case of the W2000 wave propagating through the W2000 winds (Figure 7a).

The results obtained for the Z93 wave, shown in Figure 7b, appear to be more influenced by mean winds than the W2000 wave. This is especially so for altitudes between about 90 km and 105 km altitude, where values of $\varphi(w'p')$ are the most negative for the HWM93 winds at 0400 LT, and differ by as much as 20° from the windless values of $\varphi(w'p')$. This implies that reflection is stronger in the case of the HWM winds at 0400 LT, which may be substantiated by comparison with the m_{fw}^2 results presented earlier: the small values of m_{fw}^2 occurring above about 93 km altitude for the HWM winds at 0400 LT (Figure 6b) imply increased reflection from this high- altitude region (compared to the other results shown in this figure). Notice also that for this set of wave parameters, the W2000 winds decrease the strength of reflection (as inferred from values of $\varphi(w'p')$) below about 95 km altitude and have little influence above that altitude. Although increased reflection is evident for the HWM93 winds at lower altitudes and for local times earlier than 0400 LT, the effect of the change in mean winds is to change the values of $\varphi(w'p')$ by no

(Figure 6b). For the W2000 wave parameters (Figure 6a), in the case of no winds, values of m_{fw}^2 are slightly less than 2×10^{-8} m^{-2} in the approximate height range $87-92.5$ km. It is also evident that m_{fw}^2 varies more rapidly with altitude than m_{WKB}^2 (see Figure 5a), especially below 95 km altitude. The inclusion of winds significantly modifies values of m_{fw}^2. The smallest values of m_{fw}^2 now occur near 88 km altitude for the HWM winds evaluated at 0000 LT ($\sim$1.2 $\times$ 10^{-8} m^{-2}) and near 82 km altitude for the W2000 winds ($\sim$1.3 $\times$ 10^{-8} m^{-2}). Differences between the results presented in Figure 5a with those presented in Figure 6a exist over certain altitude ranges, and these specific altitude ranges are dependent on the winds used in the simula-

Table 2. Phase of η ($\varphi(\eta)$, in Degrees) for the O$_2$ Atmospheric Airglow Obtained for Two Different Sets of Wave Parameters, and for Propagation Without Winds and With Winds, and Obtained Using the Full-Wave Model and a WKB Model

	Walterscheid Wave		Zhang Wave	
	Full Wave	WKB	Full Wave	WKB
No winds	−33.2	−39.5	−23.0	−26.3
W2000	−33.7	−41.7	−22.8	−27.2
HWM 0000 LT	−30.0	−39.4	−20.4	−27.0
HWM 0200 LT	−32.4	−38.8	−21.9	−26.3
HWM 0400 LT	−36.9	−37.6	−18.7	−24.7

Table 3. Phase of η ($\varphi(\eta)$, in Degrees) for the OH Meinel Airglow Obtained Using the Full-Wave Model and the WKB Model (in Parentheses) for Two Different Sets of Wave Parameters, and for Propagation Without Winds and With Winds, and for the Cases of Including Chemistry and Dynamics or Dynamics Only[a]

| | Walterscheid Wave | | Zhang Wave | |
	Chem-Dyn	Dyn Only	Chem-Dyn	Dyn Only
No winds	−133.5 (−131.5)	−3.2 (−4.2)	−142.7 (−149.8)	−0.3 (−1.2)
W2000	−135.3 (−143.2)	−2.0 (−2.3)	−149.5 (−158.4)	1.6 (−1.5)
HWM 0000 LT	−134.1 (−136.1)	−2.0 (−3.4)	−138.9 (−150.8)	0.8 (−0.9)
HWM 0200 LT	−135.9 (−132.1)	−4.2 (−4.8)	−144.2 (−154.4)	0.0 (−1.3)
HWM 0400 LT	−137.9 (−124.5)	−10.7 (−8.5)	−165.2 (−150.8)	−2.7 (−4.0)

[a] See text for further details.

more than about 10°. The smallest values of $\varphi(w'p')$ obtained are about −45° near 87 km altitude.

We have also calculated the phase of Krassovsky's ratio, $\varphi(\eta)$, using our full-wave and WKB models, for the W2000 and Z93 sets of wave parameters, both with and without the inclusion of mean winds. These results are summarized in Table 2 for the O_2 atmospheric airglow and in Table 3 for the OH Meinel airglow.

For the O_2 atmospheric airglow (Table 2) we note, for comparative purposes, that the value of $\varphi(\eta)$ deduced from the observations of Z93 was approximately zero, while *Hecht et al.* [1993] found that $\varphi(\eta) \leq 30°$ An important feature of the results shown in Table 2 is that values of $\varphi(\eta)$ are always negative, meaning that temperature fluctuations are leading airglow brightness fluctuations. Typically, $\varphi(\eta)$ is $\sim -30°$, in approximate agreement with the observations described by W2000. Another important feature of the results shown in Table 2 is that values of $\varphi(\eta)$ derived from the full-wave model are consistently less negative (closer to zero) than those derived from the WKB model. Therefore one can conclude that reflection is influencing (slightly) values of $\varphi(\eta)$ derived from the full-wave model. The largest difference between the full-wave and WKB-derived values of $\varphi(\eta)$ (of $\sim 8°$) occurs for the W2000 wave parameters and the W2000 winds.

For the W2000 set of wave parameters for the O_2 atmospheric airglow, derived values of $\varphi(\eta)$ are least negative (closest to zero) for the HWM93 winds at 0000 LT (for the full-wave model) and for the HWM93 winds at 0400 LT (for the WKB model). For the Z93 set of wave parameters, $\varphi(\eta)$ is least negative (closest to zero) for the HWM93 winds at 0400 LT (for both models). It is apparent that values of $\varphi(\eta)$ derived for the Z93 wave are consistently closer to zero than values of $\varphi(\eta)$ derived for the W2000 wave. The largest difference occurs for the full-wave model results using the HWM93 winds at 0400 LT, where $\varphi(\eta)$ derived using the W2000 set of wave parameters (−36.9°) is about 18° smaller than the value derived using the Z93 set of wave parameters (−18.7°). The results presented in Table 2 show that differences between values of $\varphi(\eta)$ derived for the two different waves are larger than differences associated with using different mean winds. Therefore these results show that derived values of $\varphi(\eta)$ depend more on which set of wave parameters are used rather than which mean wind profile is used.

Values of Krassovsky's ratio, $\varphi(\eta)$, for the OH Meinel airglow are shown in Table 3. Results derived from the WKB model are shown in parentheses. In addition to the case of including both chemistry and dynamics, we also present results for the case of dynamics alone. The dynamics-only case neglects chemical coupling between different minor species in the calculation of fluctuation quantities, a procedure previously used by *Walterscheid et al.* [1987] to compare the influences of dynamics and chemistry in derived airglow fluctuations. It is noteworthy that our modeled values of $\varphi(\eta)$ for the OH airglow, including both dynamics and chemistry, are in general agreement with the values of $\sim -130°$ reported by *Hecht et al.* [1993] and *Walterscheid et al.* [2000]. The large and significant differences between values of $\varphi(\eta)$ calculated for the case of chemistry and dynamics included together and the case of dynamics alone demonstrates the importance of chemistry in the airglow fluctuations. Differences in values of $\varphi(\eta)$ derived for these two

cases are typically about −130° for the W2000 wave and about −140° to −160° for the Z93 wave. (Note that these differences are not particularly sensitive to whether the full-wave or the WKB model is used.) In the case of dynamics only, fluctuations in OH Meinel brightness and temperature tend to occur almost in phase (within less than 10°). However, the inclusion of chemistry has a significant impact on the phase of Krassovsky's ratio. Fluctuations in OH Meinel brightness lag fluctuations in temperature with phase differences that range from 134° to 165°. These phase differences are always more negative for the Z93 wave than for the W2000 wave.

As was the case for the O_2 atmospheric airglow results shown in Table 2, an important feature of the OH Meinel airglow results shown in Table 3 is that values of $\varphi(\eta)$ are always negative (temperature fluctuations lead brightness fluctuations). In the case of chemistry and dynamics included together, values of $\varphi(\eta)$ are large and negative ($< -134°$) for both sets of wave parameters, no matter which nominal set of wind profiles is employed. The most negative values of $\varphi(\eta)$ occur in the case of the HWM winds at 0400 LT, while the least negative values of $\varphi(\eta)$ occur in the case of the HWM winds at 0000 LT.

Examination of the results presented in Table 3 also shows that values of $\varphi(\eta)$ obtained using the full-wave model never differ by more than $\sim 15°$ from those calculated using the WKB model. Significantly, differences in these values arising as a result of differences in dynamics (as a consequence of using either the full-wave model versus the WKB model or the different mean winds) are far smaller than the differences associated with the inclusion of chemistry, as discussed above.

4. Discussion

We calculated the refractive index m^2 (m_{WKB}^2 using equation (1) and m_{fw}^2 using equation (2)) using two sets of inferred wave parameters (those of W2000 and Z93) and found that its value is influenced by the mean winds. For both sets of wave parameters, m_{WKB}^2 achieved a minimum in the 90 km region with the W2000 winds. For the W2000 wave, m_{fw}^2 achieved a minimum near 88 km and 82 km altitude for the HWM winds at 0000 LT and the W2000 winds, respectively. We also used our full-wave model to calculate the phase difference between vertical velocity and pressure perturbations, which would be in approximate phase quadrature if reflection were strong. Although the observed phase differences were never very large, there was some evidence for increased wave reflection in the region between about 80 and 86 km for the W2000 wave propagating in the W2000 winds. However, the absolute magnitude of $\varphi(w'p')$ never exceeded about 35°, suggesting that the wave reflection would not be strong. Nonetheless, the feasibility that some wave reflection is occurring from a region centered near 90 km altitude is supported by our derived values of m^2 for the case of the W2000 wave propagating through the W2000 winds. Wave reflection also appears to be stronger for the Z93 wave than for the W2000 wave.

Our results suggest that reflection caused by mean thermal gradients cannot by itself account for the small values of $\varphi(\eta) \sim$

$0°$ for the O_2 atmospheric airglow derived from observations by Z93. However, our derived values for the O_2 atmospheric airglow emission are not inconsistent with values of $\leq -30°$ discussed by *Hecht et al.* [1993] and *Walterscheid et al.* [2000]. We have further explored the possibility that reflections associated with mean winds could improve agreement with the observations. However, the inclusion of mean winds in our model does not allow us to reproduce the small value of $\varphi(\eta)$ for the O_2 atmospheric airglow observed by Z93.

The observations of *Hecht et al.* [1993] discussed by W2000 showed that O_2 atmospheric and OH Meinel brightness fluctuations were out of phase, which was attributed to OH temperature fluctuating out of phase with OH brightness. They noted that effects associated with the different chemical processes for the two emissions may have contributed to the brightness fluctuation phase differences, but they did not explore this possibility with any explicit modeling. Here we have explored the effects of the observed wave on the OH Meinel emission, and we conclude from this modeling that effects associated with chemistry play a significant role in derived values of Krassovsky's ratio. We also examined the strength of the wave reflection and the resulting effects on the phase of Krassovsky's ratio for the O_2 atmospheric emission. Our results suggest that wave reflection would not be strong enough by itself to explain the observed phase difference between the O_2 atmospheric and OH Meinel emissions observed by W2000 because phase differences between vertical velocity and pressure fluctuations never attain magnitudes larger than $45°$.

We performed calculations to determine the sensitivity of our derived results (such as airglow phases) to the assumed model inputs, including the wind profiles, the minor species number density profiles (mainly for the OH airglow), and the mean temperature profile. Changing the minor species profiles (not shown) from those representative of average conditions at $18°N$ during June (our nominal species profiles) to those representative of average conditions at $18°N$ during March had the effect of changing values of $\varphi(\eta)$ for the OH airglow by less than $20°$ and $15°$ in the case of the W2000 wave and Z93 wave, respectively. For both waves, values of $\varphi(\eta)$ calculated using the March minor species profiles were always less negative than those obtained using the June minor species profiles. Derived values of $\varphi(\eta)$ did not appear to be so sensitive to the assumed mean temperature profile. At the low latitude of the AIDA observations ($18°N$), seasonal temperature variations should not be large and tidal temperature variations would be more important. However, derived values of $\varphi(\eta)$ for the OH and O_2 atmospheric airglow emissions never changed by more than about $5°$ from their nominal values when local times in the MSIS model (which provides a measure of tidal temperature influences) were varied.

The nominal mean wind profiles we have used are rather smooth and generally have associated large Richardson numbers. In contrast, the real atmosphere generally exhibits a multitude of motions of different temporal and spatial scales, sometimes revealing large wind shears that have associated small Richardson numbers [e.g., *Larsen*, 2000]. To investigate the sensitivity of our derived results to the nominal winds used, we repeated our analyses using a wind profile that was the sum of a sinusoidal wind profile and each (in turn) of our nominal wind profiles. The sinusoidal wind profile characterized a packet, with an adjustable characteristic vertical wavelength, maximum amplitude, height of maximum amplitude, and vertical decay scale length. A maximum amplitude of 20 m s^{-1} was used, and vertical wavelengths were varied between 5 km and 30 km. We found that the largest changes in values of $\varphi(\eta)$ occurred when the characteristic vertical wavelength of the imposed mean wind perturbation was about 10 km, which is comparable to the thickness of the airglow emission profiles. Under such conditions and for the W2000 wave, values of $\varphi(\eta)$ were reduced by up to about $16°$ and $14°$

from their nominal values for the OH and O_2 atmospheric airglow emissions, respectively. The corresponding effect on values of $\varphi(\eta)$ for the Z93 wave were smaller, being typically $13°$ and $5°$ for the OH and O_2 atmospheric airglow emissions, respectively. Although Richardson numbers were larger for the sinusoidal wind having smaller characteristic vertical wavelengths (5 km), the effect on $\varphi(\eta)$ was not so large due to cancellation effects in the perturbation VER (not shown).

Our sensitivity studies reveal that values of $\varphi(\eta)$ for the OH airglow emission are always large and negative. These values of $\varphi(\eta)$, obtained by including both dynamics and chemistry, never change by more than about $20°$ from their nominal values. However, values of $\varphi(\eta)$ obtained by including dynamics alone can differ by as much as $130°$ from values of $\varphi(\eta)$ obtained including both chemistry and dynamics. Therefore for our simulations and for the two sets of wave parameters considered, we find that chemistry is the single most important process responsible for the large, negative values of $\varphi(\eta)$ for the OH airglow emission.

In addition to the results presented and discussed here, we also simulated the airglow response to gravity waves propagating through an atmosphere characterized by zero winds below some arbitrary reference altitude (which was varied between 100 km and 130 km altitude) and large, constant winds (zero shear) above that altitude. This wind profile was not intended to represent actual mean winds in the atmosphere (it is completely unrealistic); instead, it was used to facilitate strong wave reflection. In this case, the winds were chosen to be large ($\sim$200 m s^{-1}) and in a direction opposite to the propagation direction of the waves so that the waves approached evanescence above the reference altitude. When values of $\varphi(w'p')$ became relatively large ($\sim$70$°$), we found that values of $\varphi(\eta)$ for the O_2 atmospheric airglow emission became less negative (approached zero), while values of $\varphi(\eta)$ for the OH airglow emission became more negative and approached $-\pi$. These results demonstrate the effect of strong reflection on derived values of $\varphi(\eta)$. However, reflection is never likely to be this large for the W2000 and Z93 waves simply because realistic winds do not resemble this hypothetical wind profile. Additionally, these results were obtained for a very specific choice of wind magnitude and reference height, and similar results were not generally obtained using this approach. A similar wind profile shape has been previously used by *Hickey* [2001] to study the response of the airglow to ducted gravity waves. In that particular study, the waves considered had shorter horizontal wavelengths than those considered here, and were therefore more likely to be ducted because their vertical wavelengths were not so large as those considered here. In contrast to the results discussed here, strong reflection was generally obtained for a range of wave parameters in the work of *Hickey* [2001].

The dynamical (full wave) and chemistry models are both linear, steady-state models. However, the real atmosphere is more characterized by transient gravity wave packets interacting with the airglow to produce a nonlinear response [*Hickey et al.*, 2000b; *Hickey and Walterscheid*, 2001]. In this case we may expect that the airglow response would be less ideal than that of *Hines and Tarasick* [1994]. However, time-dependent, nonlinear effects are beyond the objectives of the present study.

Hickey et al. [1993] found that their airglow results (i.e., values of $\varphi(\eta)$ for the O_2 atmospheric airglow) for this wave were not sensitive to the eddy diffusion in the model due to the large phase speed of the wave ($\sim$160 m s^{-1} for Z93 and $\sim$110 m s^{-1} for W2000). Their results also suggested a general lack of sensitivity to some of the chemical kinetic parameters used in the model. The model results of *Makhlouf et al.* [1995], which pertain to the OH nightglow, suggest that the use of a brightness-weighted temperature will produce values of $\varphi(\eta)$ which are several degrees smaller than those obtained using either the Doppler temperature or the rotational temperature. These differences are relatively

small and would not significantly impact our OH results. Because O_2 atmospheric simulations were not performed by *Makhlouf et al.* [1995], it is unclear how our O_2 atmospheric airglow results would be affected by the use of a different airglow temperature formulation.

Finally, we also used our full-wave model to calculate a reflectivity index $R = |dm/dz|/m^2$, where m is the vertical wave number defined in (2). Values of $R = 1$ imply the validity of the WKB approximation, while values of $R \geq 1$ usually indicate failure of the WKB approximation [*Einaudi and Hines*, 1971]. We obtain values of R (not shown) which never exceed 0.9 and 1.8 for the W2000 and Z93 waves, respectively (using our nominal winds profiles), implying that the WKB approximation may be a reasonable approximation for the W2000 wave and that it may be a bad approximation for the Z93 wave.

5. Conclusion

We have used a numerical full-wave model and a WKB model, each combined with a steady-state model of the airglow response to gravity waves, to simulate the O_2 atmospheric and OH airglow response to a large-scale gravity wave observed during the AIDA campaign in 1989. Two sets of wave parameters derived from previous studies were used. In one of the previous studies [*Zhang et al.*, 1993a] the airglow temperature and brightness were observed to fluctuate in phase for the O_2 atmospheric airglow, but our model cannot reproduce this small phase difference, despite our investigation of several different wind profiles in the model. The small phase differences do not appear to be related to strong wave reflection because our results suggest that reflection is not strong in the airglow region. In another previous study [*Hecht et al.*, 1993], the airglow temperature and brightness were observed to fluctuate with a phase difference of $\leq 30°$ for the O_2 atmospheric airglow, and our model results are not inconsistent with this. For the OH airglow, *Hecht et al.* [1993] found that the airglow temperature and brightness were observed to fluctuate with a phase difference of $\leq 130°$, and our model can produce similar values provided chemistry is included with the dynamics.

Our derived phase differences between airglow temperature and brightness fluctuations were large and negative, a result that reasonably mimics the observations. Extensive simulation tests have revealed that this large, negative phase of Krassovsky's ratio is a consequence of the OH chemistry. Dynamics alone cannot reproduce these phases. Additionally, extensive simulations also suggest that the effects of reflection are not strong. Therefore we conclude that the out-of-phase relation between OH airglow and temperature fluctuations is a result of the effects of chemistry. This also largely explains the observed phase relation between brightness fluctuations of the OH and O_2 atmospheric airglow emissions discussed by *Walterscheid et al.* [2000].

Appendix A

We have modeled fluctuations in the OH nightglow using the set of chemical reactions and species listed below in Table A1. This reaction set and kinetic coefficients are those applicable to the (6-2) band of the OH Meinel nightglow, which is most relevant to the observations described by *Walterscheid et al.* [2000]. The reaction rates pertaining to the excited OH (OH*) have been extensively discussed by *Adler-Golden* [1997], and references therein, and are not discussed further here.

Fluctuations in these minor species (O, O_3, H, HO_2, OH($\nu = 0$), and OH*($\nu = 6$)) are calculated using the method described in earlier papers [*Walterscheid et al.*, 1987; *Hickey*, 1988], with fluctuation quantities in the major gas calculated using our full-wave model. The simulation of fluctuations in OH (6-2) airglow brightness and the associated brightness-weighted temperature and

Krassovsky's ratio then proceeds using the approach discussed by *Schubert and Walterscheid* [1988], *Hickey et al.* [1997], and *Schubert et al.* [1999].

Table A1. Chemical Reactions and Kinetic Constants Used to Describe Fluctuations of the OH Airglow

Reaction	Rate[a]	Reference
(R1) O+OH → H+O_2	4×10^{-11}	*Winick* [1983]
(R2) H+O_2+M → HO_2+M	2.1×10^{-32} exp(290/T)	*Winick* [1983]
(R3) O+HO_2 → OH+O_2	4×10^{-11}	*Winick* [1983]
(R4) O+O+M → O_2+M	4.7×10^{-33} $(300/T)^2$	*Campbell and Gray* [1973]
(R5) O+O_2+M → O_3+M	1.0×10^{-34} exp(510/T)	*Winick* [1983]
(R6) H+O_3 → OH*+O_2	$0.03 \times 1.4 \times 10^{-10}$ exp(470/T)	*Winick* [1983] and *Adler-Golden* [1997]
(R7) OH* → OH+$h\nu$	1.609	Adler-Golden
(R8) OH*+O_2 → OH+O_2	3.0×10^{-12}	Adler-Golden
(R9) OH*+N_2 → OH+N_2	9.1×10^{-14}	Adler-Golden
(R10) OH*+O → H+O_2	2×10^{-10}	Adler-Golden

[a] Rate constants are in units of cm^6 s^{-1} for termolecular reactions, cm^3 s^{-1} for bimolecular reactions, and s^{-1} for (R7).

References

Adler-Golden, S., Kinetic parameters for OH nightglow modeling consistent with recent laboratory measurements, *J. Geophys. Res.*, *102*, 19,969, 1997.

Campbell, I. M., and C. N. Gray, Rate constant for O(^{3}P) recombination and association with N(^{4}S), *Chem. Phys. Lett.*, *18*, 607, 1973.

Einaudi, F., and C. O. Hines, WKB approximation in application to acoustic-gravity waves, *Can. J. Phys.*, *48*, 1458, 1971.

Garcia, R. R., and S. Solomon, The effects of breaking gravity waves on the dynamics and chemical composition of the mesosphere and lower thermosphere, *J. Geophys. Res.*, *90*, 3850–3868, 1985.

Hecht, J. H., T. J. Kane, R. L. Walterscheid, C. S. Gardner, and C. A. Tepley, Simultaneous nightglow and Na lidar observations at Arecibo during the AIDA-89 campaign, *J. Atmos. Sol. Terr. Phys.*, *55*, 409, 1993.

Hecht, J. H., R. L. Walterscheid, M. P. Hickey, and S. J. Franke, Climatology and modeling of quasi-monochromatic atmospheric gravity waves observed over Urbana, Illinois, *J. Geophys. Res.*, *106*, 5181, 2001.

Hedin, A. E., Extension of the MSIS thermosphere model into the middle and lower atmosphere, *J. Geophys. Res.*, *96*, 1159, 1991.

Hedin, A.E., et al., Empirical wind model for the upper, middle, and lower atmosphere, *J. Atmos. Sol. Terr. Phys.*, *58*, 1421, 1996.

Hickey, M. P., Effects of eddy viscosity and thermal conduction and Coriolis force in the dynamics of gravity-wave-driven fluctuations in the OH nightglow, *J. Geophys. Res.*, *93*, 4077, 1988.

Hickey, M. P., Airglow variations associated with nonideal ducting of gravity waves in the lower thermosphere region, *J. Geophys. Res.*, in press, 2001.

Hickey, M. P., and K. D. Cole, A quartic dispersion equation for internal gravity waves in the thermosphere, *J. Atmos. Sol. Terr. Phys.*, *49*, 889, 1987.

Hickey, M. P., and R. L. Walterscheid, A note on gravity-wave-driven volume emission rate weighted temperature perturbations inferred from O_2 atmospheric and O I 5577 airglow observations, *J. Geophys. Res.*, *104*, 4279, 1999.

Hickey, M. P., and R. L. Walterscheid, Secular variations of O I 5577 Å airglow in the mesopause region induced by transient gravity wave packets, *Geophys. Res. Lett.*, *28*, 701, 2001.

Hickey, M. P., G. Schubert, and R. L. Walterscheid, Gravity-wave-driven fluctuations in the O_2 atmospheric (0-1) nightglow from an extended, dissipative emission region, *J. Geophys. Res.*, *98*, 13,717, 1993.

Hickey, M. P., R. L. Walterscheid, M. J. Taylor, W. Ward, G. Schubert, Q. Zhou, F. Garcia, M. C. Kelley, and G. G. Shepherd, Numerical simulations of gravity waves imaged over Arecibo during the 10-day January 1993 campaign, *J. Geophys. Res.*, *102*, 11,475, 1997.

Hickey, M. P., M. J. Taylor, C. S. Gardner, and C. R. Gibbons, Full-wave modeling of small-scale gravity waves using Airborne Lidar and Observations of the Hawaiian Airglow (ALOHA-93) O(^{1}S) images and coincident Na wind/temperature lidar measurements, *J. Geophys. Res.*, *103*, 6439, 1998.

Hickey, M. P., R. L. Walterscheid, and G. Schubert, Gravity wave heating and cooling in Jupiter's thermosphere, *Icarus*, *148*, 266, 2000a.

Hickey, M. P., R. L. Walterscheid, and P. G. Richards, Secular variations of atomic oxygen in the mesopause region induced by transient gravity wave packets, *Geophys. Res. Lett.*, *27*, 3599, 2000b.

Hines, C. O., Internal gravity atmospheric waves at ionospheric heights, *Can. J. Phys.*, *38*, 1441, 1960.

Hines, C. O., and D. W. Tarasick, Airglow response to vertically standing gravity waves, *Geophys. Res. Lett.*, *21*, 2729, 1994.

Holton, J. R., *The Dynamic Meteorology of the Stratosphere and Mesosphere*, Am. Meteorol. Soc., Boston, Mass., 1975.

Krassovsky, V. I., Infrasonic variations of OH emission in the upper atmosphere, *Ann. Geophys.*, *28*, 739, 1972.

Larsen, M. F., Coqui2: Mesospheric and lower thermospheric wind observations over Puerto Rico, *Geophys. Res. Lett.*, *27*, 445, 2000.

Makhlouf, U. B., R. H. Picard, and J. R. Winick, Photochemical-dynamical modeling of the measured response of airglow to gravity waves, 1, Basic model for OH airglow, *J. Geophys. Res.*, *100*, 11,289, 1995.

Schubert, G., and R. L. Walterscheid, Wave-driven fluctuations in OH nightglow from an extended source region, *J. Geophys. Res.*, *93*, 9903, 1988.

Schubert, G., R. L. Walterscheid, and M. P. Hickey, Gravity-wave-driven fluctuations in OH nightglow from an extended, dissipative emission region, *J. Geophys. Res.*, *96*, 13,869, 1991.

Schubert, G., R. L. Walterscheid, M. P. Hickey, and C. A. Tepley, Theory and observations of gravity-wave-induced fluctuations in the O I (557.7 nm) airglow, *J. Geophys. Res.*, *104*, 14,915, 1999.

Strobel, D. F., Constraints on gravity wave induced diffusion in the middle atmosphere, *Pure Appl. Geophys.*, *130*, 533, 1989.

Taylor, M. J., M. A. Hapgood, and P. Rothwell, Observations of gravity wave propagation in the OI (557.7 nm), Na (589.2 nm) and the near infrared OH nightglow emission, *Planet. Space Sci.*, *35*, 413, 1987.

Walterscheid, R. L., G. Schubert, and J. M. Straus, A dynamical-chemical model of wave-driven fluctuations in the OH nightglow, *J. Geophys. Res.*, *92*, 1241, 1987.

Walterscheid, R. L., J. H. Hecht, R. Vincent, I. M. Reid, J. Woithe, and M. P. Hickey, Analysis and interpretation of airglow and radar observations of quasi-monochromatic gravity waves in the upper mesosphere and lower thermosphere over Adelaide, Australia (35°S, 138°E), *J. Atoms. Sol. Terr. Phys.*, *61*, 461, 1999.

Walterscheid, R. L., J. H. Hecht, F. T. Djuth, and C. A. Tepley, Evidence of reflection of a long-period gravity wave in observations of the nightglow over Arecibo on May 8–9, 1989, *J. Geophys. Res.*, *105*, 6927, 2000.

Winick, J. R., Photochemical processes in the mesosphere and lower thermosphere, in *Solar-Terrestrial Physics*, edited by R. L. Carovillano and J. M. Forbes, pp. 677–732, D. Reidel, Norwell, Mass., 1983.

Zhang, S., R. N. Peterson, R. H. Wiens, and G. G. Shepherd, Gravity waves from O$_2$ nightglow during the AIDA '89 Campaign, I, Emission rate/temperature observations, *J. Atmos. Sol. Terr. Phys.*, *54*, 355, 1993a.

Zhang, S., R. H. Wiens, and G. G. Shepherd, Gravity waves from O$_2$ nightglow during the AIDA '89 Campaign, II, Numerical modeling of the emission rate/temperature ratio, η, *J. Atmos. Sol. Terr. Phys.*, *54*, 377, 1993b.

M. P. Hickey, Department of Physics and Astronomy, Clemson University, 308 Kinard Laboratory, Clemson, SC 29634-0978, USA. (hickey@hubcap.clemson.edu)